

Effect of 80 MeV oxygen ion beam irradiation on the properties of CdTe thin films

R. Sathyamoorthy · S. Chandramohan ·
P. Sudhagar · D. Kanjilal · D. Kabiraj ·
K. Asokan · K. P. Vijayakumar

Received: 25 May 2006 / Accepted: 10 November 2006 / Published online: 25 April 2007
© Springer Science+Business Media, LLC 2007

Abstract Polycrystalline CdTe thin films were irradiated with 80 MeV oxygen (O^{6+}) ions for various fluences and its effect on the composition, structure, surface topography and optical properties have been investigated. The as-grown films are found to be slightly Te-rich in composition and there is no significant change in the composition after irradiation. X-ray diffraction analysis shows a high degree of crystallite orientation along the (111) plane of cubic phase CdTe. Upon irradiation a large decrease in intensity of the (111) plane and a small shift in the peak position has been resulted. The shift in the peak position is correlated with the change in the residual stress. The surface roughness of the films get increased after irradiation. A decrease in the grain size was observed after irradiation due to ion-induced recrystallization. The optical band gap energy decreased from 1.53 eV for as-grown film to 1.46 eV upon irradiation. The photoluminescence (PL) spectrum is dominated by the defect band and the effect of irradiation has been discussed and correlated with the observed change in the XRD peak position and optical band gap.

Introduction

Narrow band II–VI compound semiconductors exhibit many interesting solid-state phenomena of considerable practical importance and have been one of the great success stories of recent technological research. The compound cadmium telluride (CdTe) is of interest for the fabrication of low cost and high efficient devices such as solar cells, gamma and X-ray room-temperature nuclear detectors and electro-optic modulators [1–3]. The fast progress in photovoltaic (PV) technology widely utilizes this material as an efficient absorber in CdTe/CdS solar cells because of its direct band gap of 1.5 eV, high optical absorption as high as 10^5 cm^{-1} [4] and a small thickness needed to absorb photons (10 \AA can absorb 90% of photons with energy higher than the band gap) [5]. The maximum reported efficiency of CdTe/CdS solar cells is 16.5% [6]. Most of the high efficient devices make use of the CdCl₂ post deposition treatment in order to promote grain growth, interdiffusion at the junction and to reduce structural defects. The interdiffusion between CdTe and CdS is believed to be responsible for overcoming the lattice mismatch $\varepsilon = (a_{\text{CdTe}} - a_{\text{CdS}})/a_{\text{CdS}} = 9.7\%$ that exists at the metallurgical interface. Otherwise, the lattice mismatch is large enough to generate structural defects such as intrinsic stacking faults and dislocations at the interface, which then introduce interface states at the junction [7].

MeV ion beam irradiation has been exploited by researchers in different ways in the field of Materials Science. The ions while passing through a material interact with the surrounding atoms near its trajectory mainly through intense electronic excitation and ionization of the atoms around its path. The energy transferred from the ions to the atoms and subsequent relaxation of the system defines the amount and region of modification of the

R. Sathyamoorthy (✉) · S. Chandramohan ·
P. Sudhagar
PG and Research Department of Physics, Kongunadu Arts &
Science College, Coimbatore, Tamilnadu 641 029, India
e-mail: rsathya59@yahoo.co.in

D. Kanjilal · D. Kabiraj · K. Asokan
Inter University Accelerator Centre (IUAC), Aruna Asaf Ali
Marg, New Delhi 110 067, India

K. P. Vijayakumar
Department of Physics, Cochin University of Science and
Technology, Cochin, Kerala 682 022, India

properties of the materials. By suitably controlling the energy, flux and type of the ion the properties of the target material can be modified in a controlled way. More specifically, the interaction of ion with materials is the deciding factor in the ion beam induced materials modification. Recently, Ion Beam Mixing is widely used for generating new phases in different multilayers Fe/Si, Co/Si, Cu/W and In/Se, etc [8–11]. The hypothesis that the ion beam mixing is due to interdiffusion at the interface motivated us to study the effect of high-energy ion irradiation on interdiffusion in CdTe/CdS heterojunctions.

When solar cells are used in space for power generation, the main concern is the degradation due to damage caused by high-energy particles like electrons and protons. The performance of CdTe/CdS devices upon proton and electron irradiation has been studied independently by Romeo et al. [12] and Batzner et al. [13]. Still relatively new to CdTe/CdS device processing is the use of MeV ion irradiation, although this application has received considerable attention for other semiconductors such as ZnO, Cu₂O, In₂S₃ and amorphous chalcogens (GeSe, SeSbIn), etc [14–18]. Hence, investigation should be paid not only at the interface but also significantly on the individual layers constituting the devices. Therefore we aimed to systematically study the effect of ion beam irradiation on CdTe and CdS films and their junctions. This paper is first of its kind and reports the effect of 80 MeV oxygen ion irradiation on the properties of CdTe thin films. In the present work the irradiation induced surface roughening, modification of residual stress and optical properties has been reported. The experimental results show significant modification in the properties as a function of ion fluence.

Experimental details

CdTe thin films were deposited on chemically cleaned glass substrates using a conventional vacuum coating unit. The starting material (99.999% pure stoichiometric CdTe powder) was evaporated from a molybdenum boat at a pressure of 6×10^{-6} mbar. The thickness of the film was monitored in situ by quartz crystal thickness monitor and is about 1 μm . Ion beam irradiation was done using 15 UD Pelletron tandem accelerator. Films of 1 cm^2 area were mounted on a ladder in an irradiation chamber evacuated at a pressure of 10^{-6} mbar. The films were subjected to 80 MeV oxygen ion irradiation for different fluences namely 1×10^{12} , 1×10^{13} , and 1×10^{14} ions/ cm^2 . The beam current was maintained <3 pA (particle nanoampere) to avoid heating effect during irradiation. The ion beam was focused to a spot of 10 mm diameter and then scanned over an area of 1 cm^2 using magnetic scanner to achieve the dose uniformity across the sample area. The

fluence values were measured by collecting the charge falling on the sample mounted on an electrically insulated sample ladder placed in secondary electron suppressed geometry. Ladder current was integrated with a digital current integrator and the charged pulses were counted using scalar counter. The projected range of 80 MeV ions in the films calculated using SRIM-2003 (Version 2003.26) software is about 50.56 μm , which is greater than the total thickness of the film. Thus, the bombarding ions pass through the entire film and deposit in the substrate. For this energy the electronic and nuclear energy loss values are 1.202×10^2 and 7.492×10^{-2} eV/ \AA , respectively.

The films were characterized before and after irradiation to study the influence of irradiation on the film properties. The elemental analysis of the films was made by using Energy Dispersive X-ray Spectrometer (EDS), INCA Oxford, optionally attached with Scanning Electron Microscope (JEOL JSM 5600). The experiment was carried out with an accelerating voltage of 20 kV. The structural properties were studied by X-ray diffraction technique (Shimadzu XRD 6000) using CuK $_{\alpha}$ radiation. The surface morphology was investigated by scanning the surface of the films using Atomic Force Microscope (AFM) operated in tapping mode. A UV–Vis–NIR Spectrophotometer (JASCO V-570) was employed to record the optical transmittance and absorbance spectra. The PL spectra were recorded at room temperature using He–Ne laser as an excitation source ($\lambda = 632.8$ nm).

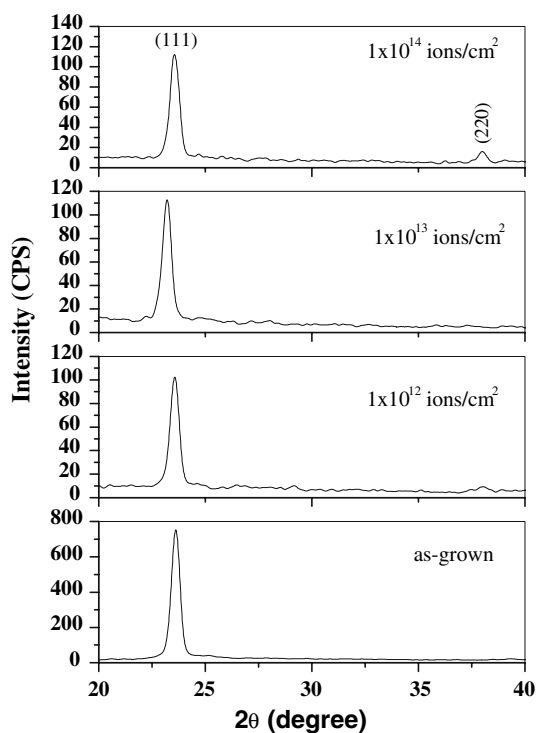
Results and discussion

Structural analysis

The study of chemical composition of the films is an important aspect because any change in elemental composition will affect the electronic properties of the material significantly. The elemental composition of the films has been studied using EDS. The qualitative analysis made on the spectra gives Cd/Te ratio as 0.93 for the as-grown film, which implies that the films are slightly Te-rich in composition. The composition of the films after irradiation has also been studied and the value of Cd/Te ratio for films irradiated with different ion fluence is given in the Table 1. It clearly shows that there is no significant change in the composition after irradiation. The X-ray diffraction patterns of as-grown and 80 MeV oxygen ion irradiated CdTe films at different fluences are shown in Fig. 1. An intense (111) reflection has seen for the as-grown film, which is due to the oriented growth of the grains along the (111) direction of cubic phase CdTe. The intensity of this peak for irradiated films decreased by a factor of five from that of the as-grown film. In general, an increase or decrease of

Table 1 Calculated structural and morphological parameters as a function of ion fluence

Fluence (ions/cm ²)	2θ (°)	FWHM (°)	d (Å)	d _{bulk} = 3.7008 Å	Stress (10 ⁹ Pa)	Cd/Te ratio (±0.03)
As-grown	23.59	0.411	3.768		0.97	0.93
1 × 10 ¹²	23.54	0.441	3.775		1.07	0.90
1 × 10 ¹³	23.18	0.425	3.833		1.91	0.92
1 × 10 ¹⁴	23.55	0.447	3.774		1.06	0.95

**Fig. 1** X-ray diffraction spectrum of as-grown and 80 MeV oxygen ion irradiated CdTe thin films

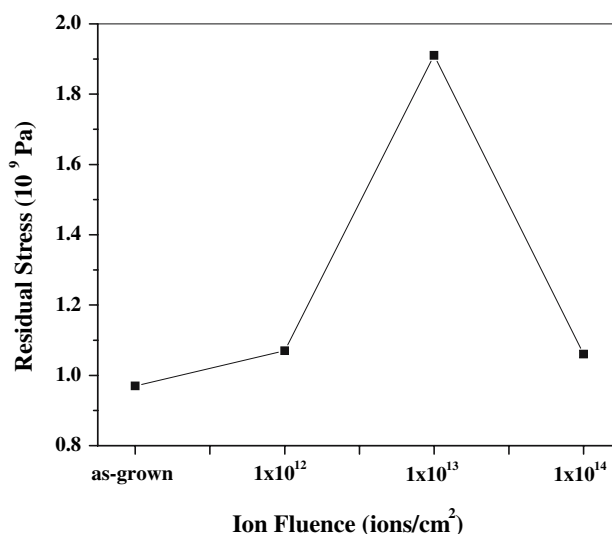
the diffraction intensity could be expected on the irradiated films due to the creation or annihilation of defects and recrystallization process during irradiation [19]. The position of (111) peak as a function of ion fluence is given in Table 1.

The X-ray diffraction data can also be used to determine internal stress in the films. A displacement of diffraction peaks from their corresponding stress-free data is an indication of development of residual stress normal to the corresponding crystal plane in the film during condensation. Almost all the films grown by any technique normally have a residual stress of certain magnitude that depends on the material and growth conditions. In a film residual stress may occur at the scale of microstructure (intergranular micro stress) as well as at the level of crystal structure (intragranular micro stress). Such stresses are, by necessity, balanced by stresses in other locations (or directions) or crystal planes within the material for an equilibrium configuration [20]. In the present work a shift in the position of

the (111) peak by an amount 0.434° towards lower diffraction angle from its corresponding powder data (2θ = 24.026°; JCPDS No. 75-2086) indicates the development of tensile stress in the as-grown films. The increased lattice *d*-spacing of the (111) plane also indicates a tensile stress normal to this plane. This residual stress arises due to the lattice mismatch between the thin film layer and underlying substrate [21, 22]. We have also observed a progressive shift in the peak position towards lower diffraction angle for irradiated films up to 1 × 10¹³ ions/cm², while the trend is quite opposite beyond this fluence. Rawat et al. [23] observed a similar relaxation in the lattice stress upon irradiation in thermally evaporated CdI₂ films subjected to argon ion irradiation. The value of the tensile stress is calculated by multiplying the strain produced, given by the expression

$$\frac{\nabla d}{d} = \frac{d(\text{observed}) - d(\text{ASTM})}{d(\text{ASTM})} \quad (1)$$

with the elastic stiffness constant of CdTe ($C_{11}=5.351 \times 10^{10}$ Pa), where ASTM stands for American Society for Testing and Materials. The estimated values of tensile stress are given in Table 1 and its variation as a function of ion fluence is depicted in Fig. 2. The figure clearly shows that the tensile stress increases with ion fluence up to 1 × 10¹³

**Fig. 2** Variation in residual stress as a function of ion fluence

ions/cm² and then shows a decreasing tendency at higher ion fluence. Variations of the stress are caused by the changes in the microstructure of the films induced by bombarding ions. There are many structure transformations that may influence on the stress in a film like creation of hillocks, shrinkage of grain boundary voids or amorphization of the film or substrate. It is very difficult to determine the exact physical process, which caused the changes of the residual tensile stress but in the present investigation the changes of the stress can be attributed to the fragmentation of grains during irradiation. It was observed from the Table 1 that the full width at half maximum (FWHM) of the (111) peak increases with ion fluence. This may be due to the irradiation induced lattice damage resulting in the decrease of the degree of (111) orientation [24].

Surface morphology

The grain size and surface morphology are most important aspects affecting the efficiency of CdTe/CdS devices irrespective of the growth procedure [25]. A parameter of easy physical interpretation used to characterize the surface morphology of thin films is its roughness, which can be considered as an inheritance of the growth process. The measured root mean square surface roughness for $5 \times 5 \mu\text{m}$ area of the as-grown sample and films subjected to irradiation at ion fluence of 1×10^{12} , 1×10^{13} ions/cm² is 6.339, 6.814, and 7.049 nm, respectively. This result indicates a consistent increase in the surface roughness with increasing ion fluence. Li et al. [26] reported an increase in efficiency of solar cells when the surface becomes more and more rough. The rougher surface will promote multiple surface reflections by reducing the energy loss due to reflectance. Thus the ion beam irradiation with selective ions can be utilized to form rougher surface (such as formation of primides). Figure 3 depicts the three-dimensional (3D) AFM images of CdTe film surface before and after irradiation. The micrograph for the as-grown film surface of $1 \mu\text{m}^2$ area shows formation of well-defined spherical grains of 80–100 nm sizes. The size of the grains has been estimated from the corresponding two-dimensional micrographs by considering more than 20 grains. After irradiation the grains seem to be more closely packed due to melting of grains followed by regrowth, which is clearly seen from Fig. 3b and c. A comparison on the micrographs infers that there is a decrease in grain size (50–60 nm) after irradiation, which may be due to ion beam induced recrystallization process.

Optical properties

The optical properties of thin films have strong correlation with the grain size and residual stress and hence the stress

generated in the films should also affect their optical spectra yielding considerable amount of defects and disorder in the films. The optical transmittance spectra of as-grown and irradiated films are shown in Fig. 4. The spectra shows the usual interference pattern of a high index film in the region of low absorption with a sharp fall of transmittance at the band edge, which is an indication that the film has good crystallinity. As can be seen from the Fig. 4 that the band edge of the irradiated films shifts towards higher wavelength with a large decrease in the transmittance which is more prominent for films irradiated at a fluence of 1×10^{14} ions/cm². But this shift is not clearly visible for those films irradiated at a fluence of 1×10^{12} and 1×10^{13} ions/cm² due to the fact that for these films the transmittance did not reach zero beyond the fundamental absorption. Figure 5 illustrates the variation of optical absorption as a function of wavelength for as-grown and irradiated films. It is seen that the spectra is not consistent with the ion fluence. For the fluences 1×10^{12} and 1×10^{13} ions/cm² the absorbance measured at wavelengths in the range 400–800 nm are lower than that of the as-grown film and shows no significant variation, while for the fluence 1×10^{14} ions/cm² the absorbance is higher. Such exponential increase of absorbance with wavelength is primarily due to the production of defect levels in the band gap [27] whereas the decrease in absorbance for other fluences is unclear.

In a polycrystalline material the nature of optical inter-band transitions (direct or indirect) near the absorption edge can be determined by the relation between absorption coefficient (α) and the optical energy gap (E_g). Using the standard expression for direct transition between two parabolic bands $(\alpha hv)^2 = A(hv - E_g)$, the band gap of both as-grown and irradiated films was estimated. The value of E_g is determined from an intercept on the energy axis of $(\alpha hv)^2$ versus hv plot as shown in Fig. 6 and the values are given in Table 2. The band gap energy decreases gradually with increase in ion fluence. Similar decrease in the band gap energy during irradiation has been reported on other semiconductor thin films and is due to creation of intermediate energy levels [19] and increase in the carrier concentration [28]. In the present work the observed decrease in the band gap energy is attributed to the creation of intermediate energy levels within the forbidden gap. It is worthwhile to mention here that the observed change in band gap energy may also be due to the variation in residual stress because change in lattice strain will cause modification in the electronic band structure and hence shift in the band edge.

Photoluminescence properties

The relatively open zincblende structure of CdTe should easily accommodate interstitial atoms in fact the atomic

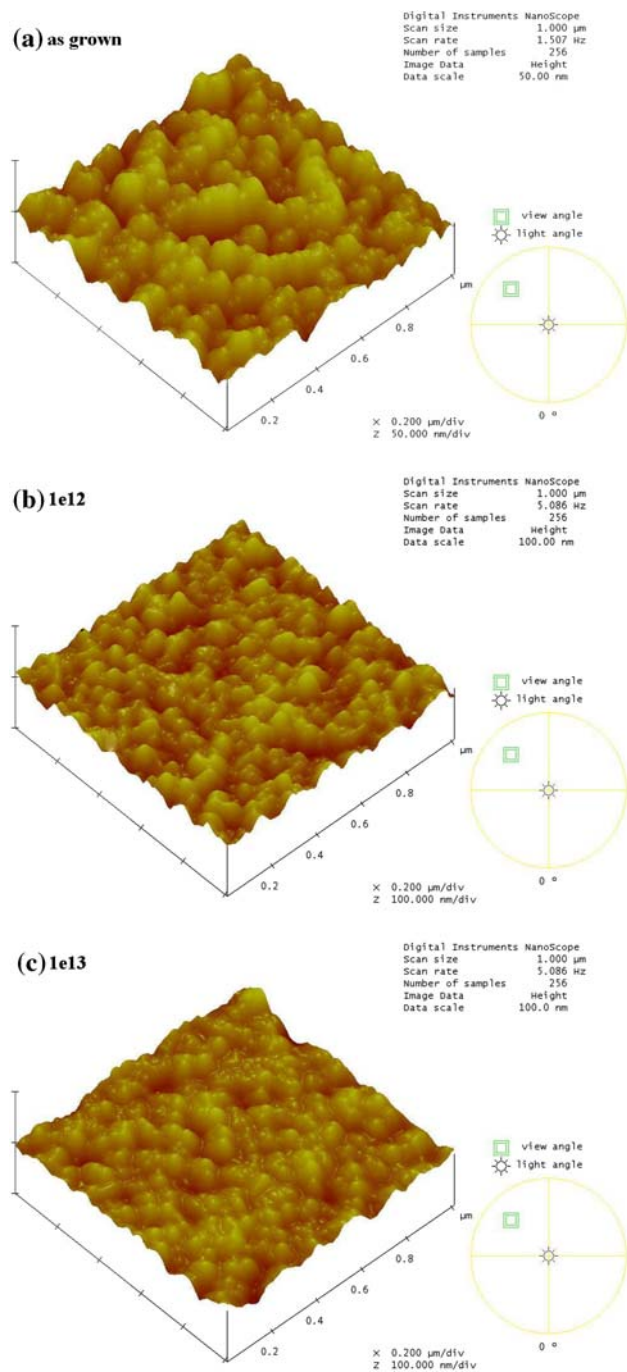


Fig. 3 Three-dimensional atomic force micrographs of as-grown and irradiated CdTe films

spacing in CdTe is larger than the spacing of most tetrahedral structures. Correspondingly, the cohesive strength of CdTe is smaller than that of most tetrahedral structures suggesting the energy of vacancy formation to be smaller and the concentration of vacancies to be relatively larger. Hence a considerable native defect density is expected in CdTe films irrespective of the growth process and post deposition treatment. Generally, PL studies have been

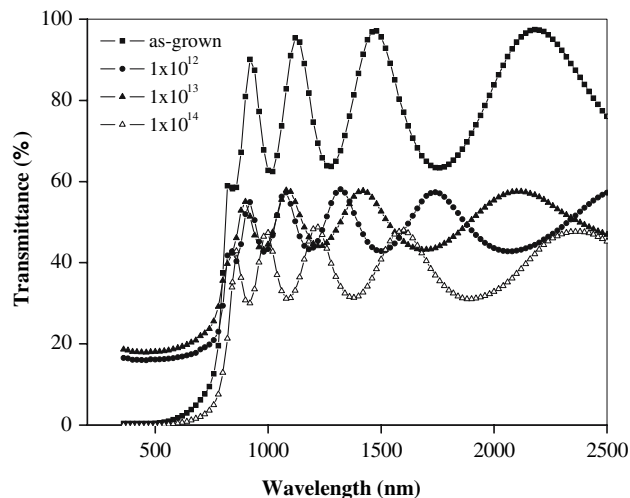


Fig. 4 Transmittance spectra of as-grown and irradiated CdTe thin films

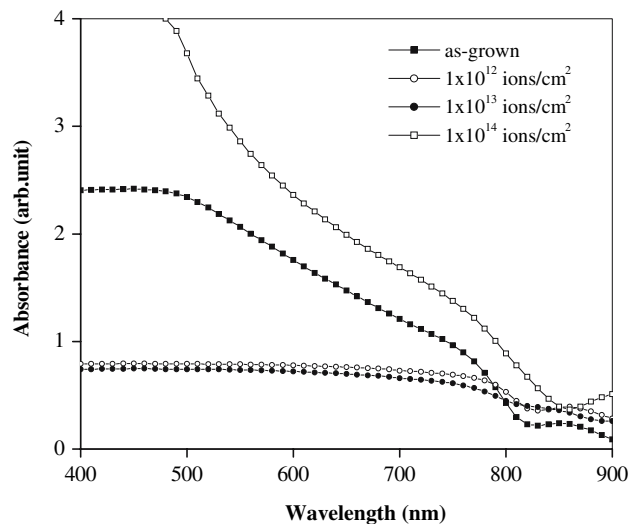


Fig. 5 Absorbance spectra of as-grown and irradiated CdTe thin films

directed towards the identification of such native defects and impurities, either through direct recombination associated with band to defect-type transitions or the recombination of excitons associated with defect centers. Figure 7 shows the PL emission spectra of as-grown and irradiated CdTe films. The spectrum of as-grown film is dominated by a broad band with twin peaks at 1.436 and 1.457 eV. In general, the 1.457 eV band has been observed between 1.4 and 1.49 eV, usually ascribed to intrinsic defects/impurities and, consequently, is known as the defect band. This includes band-acceptor ($e-A$) transitions, donor-acceptor pair (DAP) recombination and internal transitions within highly localized defects. In the present work the 1.457 eV peak is attributed to the shallow DAP transitions, the recombination

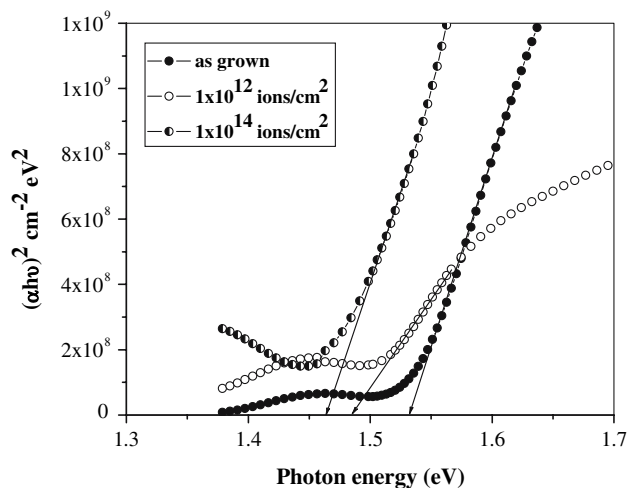


Fig. 6 Plot of $(\alpha hv)^2$ versus $h\nu$ for as grown and irradiated CdTe thin films

of free charge carrier from the conduction band with a carrier bound on an acceptor. The assignment of the peak to the DAP recombination is supported by the earlier works on CdTe single crystals and films [29–31]. The peaks observed at 1.436, 1.415, and 1.391 eV are the longitudinal-optical (LO) phonon replicas of the 1.457 eV peak. We have observed a weak band around 1.55 eV, which most probably related to cadmium vacancies (V_{Cd}) and could be associated with the transition from conduction band to V_{Cd} acceptor level [32, 33]. The EDS analysis also indicates cadmium deficiency in the films.

The major difference between the spectra of as-grown and irradiated films is the shift in the position of the defect band and change in its emission intensity. For film exposed to 1×10^{12} ions/cm² a broad feature centered at 1.492 eV is observed with a row of equidistant peaks at 1.471, 1.450, and 1.513 eV, whose energy separation is equal to the CdTe LO phonon energy of 21 meV [22, 34]. The peak at 1.513 eV, the so-called ‘shoulder’ is identified as the zero-phonon line of the DAP recombination and the peaks at 1.471 and 1.450 eV are the first and second LO phonon replicas of the band at 1.492 eV. Another weak band centered at 1.553 eV can be related to cadmium vacancies. The position of the dominant broad band for films irradi-

Table 2 The variation of optical band gap energy and defect band position with ion fluence

Ion fluence (ions/cm ²)	Band gap energy (eV) ±0.005	PL band position (eV)
As-grown	1.53	1.457
1×10^{12}	1.49	1.492
1×10^{13}	1.47	1.468
1×10^{14}	1.46	1.429

ated with 1×10^{13} and 1×10^{14} ions/cm² was observed at 1.468 and 1.429 eV, respectively, along with their phonon replicas. The decrease in intensity with the ion fluence may be due to creation of high density of defects. The shift in the position of the peak is directly correlated with the shift in the position of the (111) peak as observed in XRD spectrum. Therefore the shift in the defect band position may be either due to the variation in the residual stress or in the band gap energy. The correlation between the shift in the PL peak position and the shift in the band gap energy is in good agreement with the work of Vamsi Krishna et al. [7], where the shift in the exciton peak position is reported due to the change in the band gap of CdTe.

Conclusion

The effect of high-energy deposition in CdTe thin films has been investigated by irradiating the films with 80 MeV oxygen ions at different fluences. The composition of the films is not affected significantly whereas the structural quality is marginally affected due to irradiation. The grain size decreased due to irradiation induced recrystallization process. The morphology of the irradiated films reveals an increase in the surface roughness, which is most desirable to enhance the collection efficiency of a solar cell. The decrease in band gap energy with ion fluence suggests formation of trap levels. The defect band dominated PL spectra indicates a high density of defects in CdTe films resulting from Cd vacancies and due to the very small grain size. At higher ion fluence, the irradiation causes severe damage to the surface resulting in the decrease of the luminescence intensity. From these observations it is concluded that oxygen ion irradiation under optimum conditions could be useful for device applications.

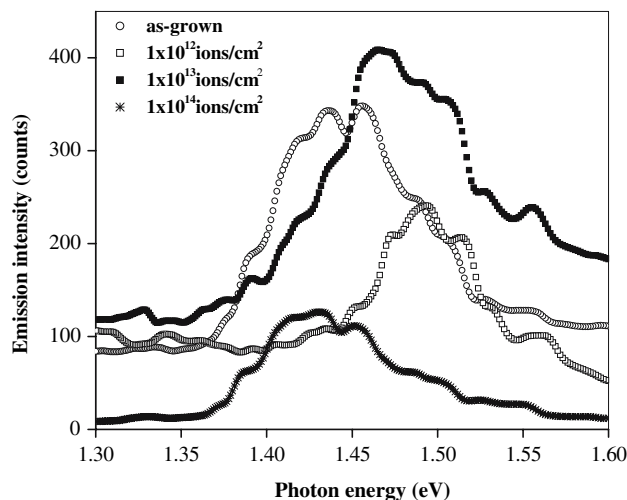


Fig. 7 Photoluminescence spectra of as-grown and irradiated CdTe thin films

Acknowledgements This work was supported by the Inter University Accelerator Centre (IUAC), New Delhi, India through the Project UFUP 34319. The authors cordially acknowledge the help extended by technical staff of Pelletron group during the irradiation experiment. The authors wish to acknowledge Mr. Ambuj Tripathi, Scientist, Inter University Accelerator Centre, New Delhi for his support to carryout the AFM measurements and Dr. D. M. Phase, Scientist and Mr. Vinay Ahire, Junior engineer, UGC-DAE Consortium for Scientific Research, Indore Centre for EDA analysis. One of the authors (RS) gratefully acknowledges University Grants Commission (UGC), New Delhi for awarding UGC-Research Award [Project No. F-30-1/2004 (SA-II)].

References

1. Leal FF, Ferreira SO, Menezes-Sobrinho IL, Faria TE (2005) *J Phys Condens Matter* 17:27
2. Cavallini A, Fraboni B, Dusi W, Hage-Ali M, Siffert P (2001) *J Appl Phys* 89:4664
3. Rams J, Sochinskii NV, Munoz V, Cabrera JM (2000) *Appl Phys A Mater Sci Process* 71:277
4. Oladeji IO, Chow L, Ferekides CS, Viswanathan V, Zhao Z (2000) *Sol Energy Mater Sol Cells* 61:203
5. Aguilar M, Oliva AI, Castro-Rodriguez R, Pena JL (1997) *J Mater Sci Mater Electron* 8:103
6. Wu X, Keane JC, Dhere RG, Dettart C, Albin DS, Duda A, Gessert TA, Asher S, Levi DH, Sheldon P (2001) In: *Proc of the 17th European Photovoltaic Solar Energy Conf., Munich, Germany*, p 995
7. Vamsi krishna K, Dutta V (2004) *J Appl Phys* 96:3962
8. Schattat B, Bolse W, Elsanousi A, Renz T (2005) *Nucl Instrum Methods Phys Res B* 230:240
9. Senthilarasu S, Sathyamoorthy R, Lalitha S, Avasthi DK (2005) *Thin Solid Films* 490:177
10. Avasthi DK, Assmann W, Nolte H, Mieskes HD, Huber H, Subramanian ET, Tripathi A, Ghosh S (1999) *Nucl Instrum Methods Phys Res B* 156:143
11. Sreekumar R, Ratheesh Kumar PM, Sudha Kartha C, Vijayakumar KP, Kabiraj D, Khan SA, Avasthi DK (2006) *Nucl Instrum Methods Phys Res B* 244:190
12. Romeo A, Batzner DL, Zogg H, Tiwari AN (2001) *Mat Res Soc Symp Proc* 668:H3.3.1
13. Batzner DL, Romeo A, Terheggen M, Dobeli M, Zogg H, Tiwari AN (2004) *Thin Solid Films* 451–452:536
14. Ratheesh Kumar PM, Sudha Kartha C, Vijaya Kumar KP, Singh F, Avasthi DK, Abe T, Kashiwaba Y, Okram GS, Kumar M, Kumar S (2005) *J Appl Phys* 97:013509
15. Balamurugan B, Mehta BR, Avasthi DK, Singh F, Arora AK, Rajalakshmi M, Raghavan G, Tyagi AK, Shivaprasad SM (2002) *J Appl Phys* 92:3304
16. Kamboj MS, Kaur G, Thangaraj R, Avasthi DK (2002) *J Phys D Appl Phys* 35:477
17. Ratheesh Kumar PM, John TT, Sudha Kartha C, Vijayakumar KP (2006) *Nucl Instrum Methods Phys Res B* 244:171
18. Jayavel P, Arokiaraj J, Soga T (2002) *Semicond Sci Technol* 17:969
19. Chaudhary YS, Khan SA, Shrivastava R, Satsangi VR, Prakash S, Avasthi DK, Dass S (2004) *Nucl Instrum Methods Phys Res B* 225:291
20. Ohring M (1992) In: *The materials science of thin film*. Academic Press, San Diego
21. Mouninho HR, Al-Jassim MM, Abulfotuh FA, Levi DH, Dippe PC, Dhere RG, Kazmerski LL (1997) *NREL/CP-523-22944*
22. Bhattacharya B, Carter MJ (1996) *Thin Solid Films* 288:176
23. Rawat RS, Arun P, Vedeshwar AG, Lee P, Lee S (2004) *J Appl Phys* 95:7725
24. Senthil K, Mangalaraj D, Narayandass SAK, Kesavamoorthy R, Reddy GLN, Sundaravel B (2001) *Physica B* 304:175
25. Contreras-Puente G, Vigil-Galan O, Vidal-Varramendi J, Cruz-Gandarilla F, Hesiquio-Garduno M, Aguilar-Hernandez J, Cruz-Orea A (2001) *Thin Solid Films* 387:50
26. Li K, Wee ATS, Linj J, Tan KL, Zhou L, Li SFY, Feng ZC, Chou HC, Kamra S, Rohatgi A (1997) *J Mater Sci Mat Electron* 8:125
27. Narayanan KL, Vijayakumar KP, Nair KGM, Thampi NS (1997) *Physica B* 240:8
28. El-Sayed SM (2004) *Nucl Instrum Methods Phys Res B* 225:535
29. Bridge CJ, Dawson P, Buckle PD, Ozsan ME (2000) *Semicond Sci Technol* 15:975
30. Seto S, Yamada S, Suzuki K (2001) *Sol Energy Mater Sol Cells* 67:167
31. Ahmad-Bitar R, Moutinho H, Abulfotuh F, Kazmerski L (1995) *Renew Energy* 6:553
32. Aguilar-Hernandez J, Contreras-Puente G, Vidal-Larramendi J, Vigil-Galan O (2003) *Thin Solid Films* 426:132
33. Mathew X, Arizmendi JR, Campos J, Sebastian PJ, Mathews NR, Jimenez CR, Jimenez MG, Silva-Gonzales R, Hernandez-Torres ME, Dhere R (2001) *Sol Energy Mater Sol Cells* 70:379
34. Ahmad-Bitar R, Arafah DE (1998) *Sol Energy Mater Sol Cells* 51:83